Transmission-Electron-Microscopy Study on Fivefold Twinned Silver Nanorods

Hanyuan Chen, Yan Gao, Huairou Zhang, Libao Liu, Hongchun Yu, Huanfang Tian, Sishen Xie, and Jianqi Li*

Beijing Laboratory of Electron Microscopy, Institute of Physics, Chinese Academy of Sciences, Beijing 100080, China

Received: May 8, 2004; In Final Form: June 2, 2004

Structural features of pentagonal Ag nanorods have been investigated by means of transmission electron microscopy (TEM). Cross-section observations directly reveal the remarkable fivefold twinning structure and related defects in this kind of nanomaterial. High-resolution TEM observations in combination with fast-Fourier processing indicate that the well-defined twinning relationship appears on at least two of the five twinning boundaries. Electron-energy-loss spectroscopy analysis on the center regions of the nanorods demonstrates that the Ag-$M_{4,5}$ peaks shift to lower energy in comparison with results from the Ag crystal.

Introduction

Nanoparticles and nanorods (nanowires) with notable microstructure have attracted much attention in recent years because they are important not only for fundamental studies but also for potential applications in the developments of nanoscale electronic and optoelectronic devices.[1] A good understanding of the microstructure properties is obviously the key point for obtaining nanoparticles and nanorods (nanowires) with desired properties. Multiple twinning, as a very special structural feature, has attracted substantial attention in studies of small nanoparticles during the last 50 years[2−6] Ino[2] first proposed a multiply twinned particle (MTP) model in small clusters for understanding decahedral and icosahedral structures. Marks et al.[4,5] reported icosahedral multiply twinned nanoparticles consisting of 20 tetrahedra twinned on their {111} planes. Recently, nanorods (nanowires) with some specific sizes, shapes, and symmetric properties have been studied. For instance, copper nanorods were prepared by the polyol process, these kind of Cu nanorods are held to be truncated decahedra with fivefold symmetry.[7] Hofmeister[8] reported certain microstructure properties of the multiply twinned silver nanoparticles with a rodlike shape. Well-defined silver nanorods (nanowires) are desirable for their optical and electronic properties.[1] Methods for preparing Ag nanorods have been reported in the literature; examples include membrane templates,[9] solid−liquid-phase arc discharge,[10] a pulsed sonochemical method,[11] and a recent novel polyol process.[12−14] There have been a few TEM studies of Ag nanorods, with most focusing on determination of the fundamental structure features.[12] Recent studies[7,12,15] suggested that this kind of metal nanorods shows a fivefold twining structure; however, no direct experimental evidence on the cross-section structure was reported to characterize this remarkable twinning nature.

In the present work, we systematically investigated the fivefold twinning structure in silver nanorods by TEM. We report for the first time the results of high-resolution TEM (HRTEM) observations and selected area electron diffraction (SAED) measurements, especially those obtained from the cross-section of Ag nanorods. The remarkable fivefold twinning structure, twinning relationship, defects, and structural distortion have been analyzed in detail. Our systematic investigations are expected to shed light on the understanding of atomic structural features of the fivefold twinned nanorods and the growth mechanism of this kind of nanomaterial.

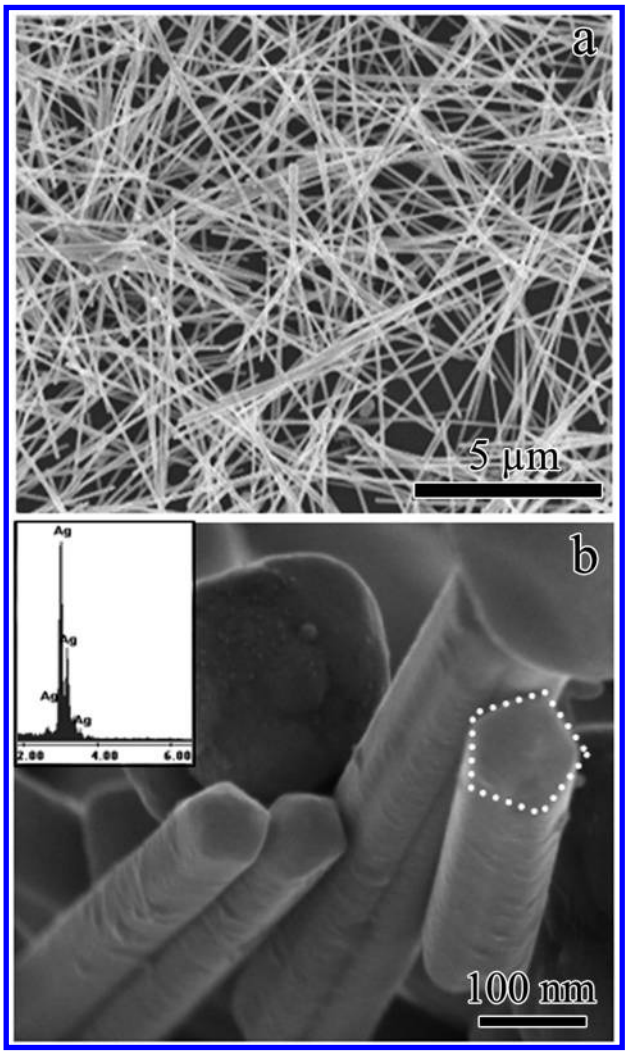

Figure 1. SEM images showing (a) the large concentration of Ag nanorods and (b) pentagonal profiles of the nanorods. The inset shows the EDX data from a nanorod.

* Corresponding author. E-mail: ljq@aphy.iphy.ac.cn. Tel: +86-10-82649524; Fax: +86-10-82649531.

10.1021/jp048023d CCC: $27.50
Published on Web 07/16/2004

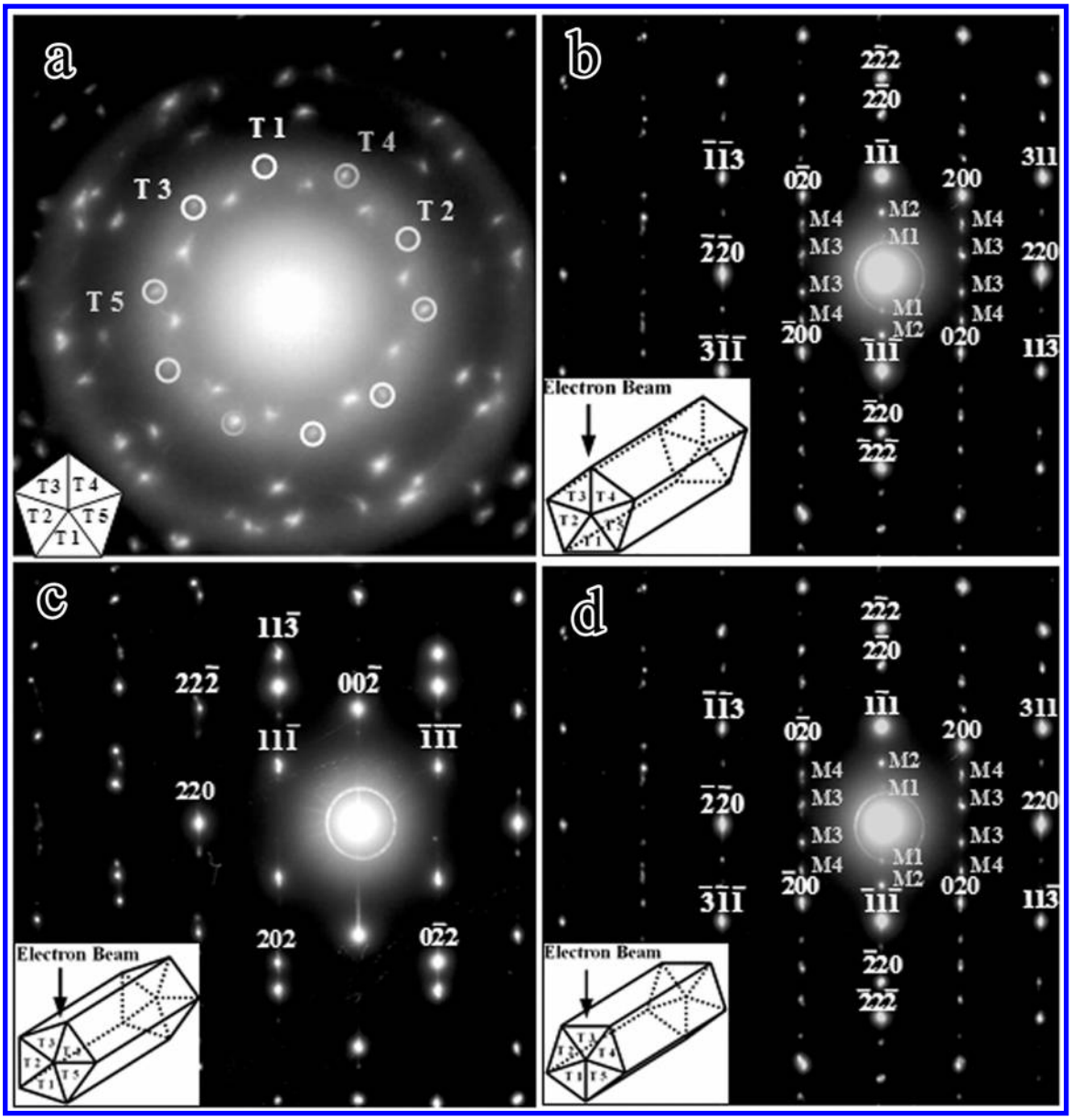

Figure 2. SAED patterns for different orientations of an Ag nanorod. The insets schematically illustrate the orientations of the nanorods, arrowheads indicate the electron beam direction. (a) The cross-section SAED showing the remarkable fivefold symmetry. (b) A significant SAED for characterizing the structure of Ag nanorods, weak spots from superimposition of the [112] and [100] zone axis are indicated. (c) SAED after a clockwise 18° rotation from Figure 2b. (d) SAED obtained after a clockwise 36° rotation showing similar properties with Figure 2b.

Methods and Materials

Materials containing a large fraction of Ag nanorods used in the present study have been synthesized by polyol reduction of silver nitrate in the presence of poly(vinylpyrrolidone) (PVP).[14] The procedure is briefly described as follows: first, 10 mL of ethylene glycol (EG) was refluxed in a three-necked round-bottom flask at 160 °C for 2 h, then 6 mL EG solution of 0.1M silver nitrate and 6 mL EG solution of 0.6 M PVP were simultaneously injected dropwise. After injection, the solution turned turbid with a gray color in about 15 min, indicating the appearance of Ag nanorods, and the reaction continued at 160 °C for about 60 min. When the reaction finished, the supernatant was removed; the gray precipitate remained. The gray precipitate contained Ag-nanorods (80%) and some other small particles. Specimens for TEM observations were prepared by two methods: (1) the powder samples were dispersed in acetone using an ultrasonic device. One droplet of Acetone, containing Ag nanorods, was dropped to the holed carbon supporting film (or microgrids). After being well dried in air, the grid was mounted on the TEM specimen holder for examination. (2) Samples for cross-section examinations in TEM were prepared by a microtome technique (microtomy) to cut the long Ag nanorods into thin slices perpendicular to the growth direction. The TEM investigations were performed on a Tecnai-F20 field-emission electron microscope with an accelerating voltage of 200 kV (Philips).

Results and Discussion

Figure 1a shows a typical scanning electron microscopy (SEM) micrograph illustrating the presence of a high concentration of Ag nanorods with random orientation. The rod length is estimated to range from 10 μm to 50 μm, and the diameter from 20 to 100 nm. Figure 1b is a SEM image with a larger magnification indicating the microstructure features and shapes of Ag nanorods. The profiles of Ag nanorods appear as clear pentagonal sections as denoted by the dashed lines. The inset

shows the energy-dispersive X-ray spectroscopy (EDX) data obtained from a typical nanorod; all peaks can be assigned to the Ag element. These results are consistent with the X-ray diffraction (XRD) data, and demonstrate that the high-purity Ag nanorods have been prepared by the polyol-reduction method.[14]

The crystallographic structure and three-dimensional crystal morphology of individual Ag nanorods are the key issues in our investigation. Figures 2a−d show several SAED patterns taken from the relevant orientations for a single Ag nanorod. The most pronounced SAED pattern obtained from the cross-section observation, as shown in Figure 2a, demonstrates that the reciprocal space of this type of Ag nanorod has a recognizable fivefold symmetry as briefly denoted by the small circles. This complex and remarkable diffraction pattern can be well interpreted by the superposition of five subcrystals related to face-centered cubic (FCC) Ag crystals with a [110] orientation, and each diffraction spot can be simply attributed to a specific subcrystal (shown as T1 to T5). It is well-known that a decahedral aggregate of unstrained FCC tetrahedral subcrystals cannot be well closed;[4] in other words, it is impossible to perfectly fill the space of a rod by five (111) twinned Ag subcrystals. The theoretical angle between two (111) planes is 70.52°, which is the wedge angle of the five tetrahedra. Since 70.52° × 5 = 352.60°, there will be an intrinsic angular gap of 7.40° to fill a 360° cycle.[4,6] However, when the sizes of the crystals is very small (for example, several nanometers or a few multiples of 10 nanometers) the extended lattice defects may help to fill the gap; the twinning crystals still yield the diffraction pattern with obvious fivefold symmetry.[16] Indeed, we observed the light splitting of peripheral diffraction spots in the pattern (see Figure 2a), and it is certainly associated with the intrinsic angular gap of 7.40°. Some typical lattice deformations of Ag subcrystals will be discussed in detail in the following discussion. Figures 2b−d show a series of SAED patterns from an Ag nanorod by tilting the rod around the growth direction [110], that is, the long axis of the nanorod. The inset diagrams schematically illustrate the tilting process in real space. An arrow in each diagram indicates, respectively, the incident-electron-beam direction. The SAED pattern shown in Figure 2b is taken from an Ag nanorod on the referenced position with T1, T3, and T4 subcrystals (as indicated in the inset) giving clear diffraction spots. Actually, the T1 subcrystal gives the diffraction pattern along the [100] zone axis direction, the T3 and T4 subcrystals give the diffraction pattern along the [112] zone axis direction.

Another striking property revealed in the Figure 2b pattern is the presence of a series of additional weak reflection spots emerging on lines perpendicular to the rod axis direction. Some of them are evidently splitting or streaking along certain directions. These weak spots can be interpreted by double-diffraction effects because of superposition of subcrystals. Therefore, we find out reflections corresponding with four types of Moiré fringes: M1, M2, M3, and M4. Parallel Moiré fringes such as as M1 and M2 are considered to result from double-diffraction at subcrystals having parallel lattice planes of different spacings, and mixed Moiré fringes such as M3 and M4 result from double-diffraction at subcrystals having a certain azimuthal rotation between lattice planes of different spacings. Hofmeister et al.[7] discussed the typical Moiré fringes possibly appearing in multiply twinned silver particles of rodlike shape.

Figure 2c shows the SAED pattern after tiling clockwise about 18° relative to Figure 2b. This relevant diffraction pattern also contains three diffracting subcrystals, with the T5 subcrystal

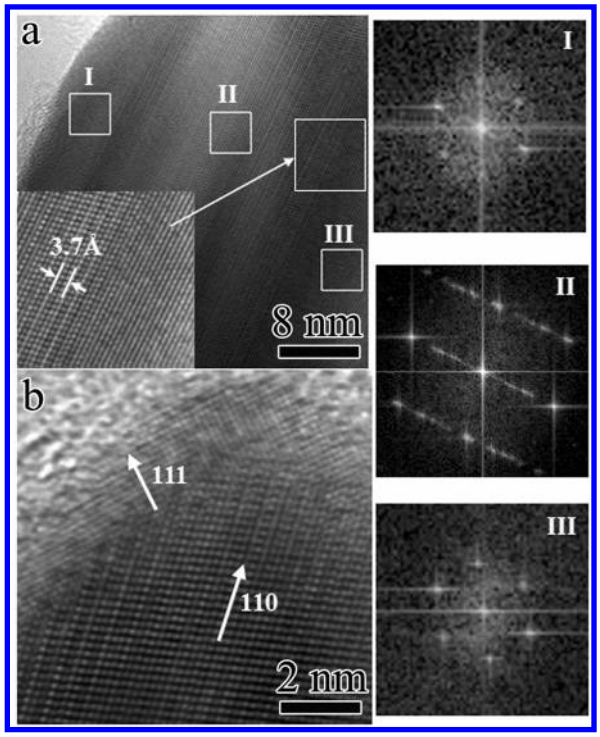

Figure 3. (a) HRTEM of an Ag nanorod with the diameter of around 20 nm. Patterns I, II, and III are respectively the FFT spectra of areas I, II, and III. (b) HRTEM image showing the structure at the end of an Ag nanorod, the image demonstrates that the rods grow along the [110] directions and are bounded by the (111) plane.

orienting along the [110] zone axis direction, the T2 and T3 subcrystals along the [111] direction. Certain reflections for the T2 and T5 subcrystals are specifically labeled in the pattern. Further titling clockwise about 18°, we can reach a position as shown in Figure 2d, which gives rise to the same diffraction pattern as the referenced SAED pattern displayed in Figure 2b. The periodic sequence for the appearance of SAED patterns in Figures 2b−d can be well understood by the pentagonal shape of the examined nanorod. This nanorod shows up an approximate fivefold symmetry and therefore yields a 360°/5 = 72° repetition in real space and a 36° repetition for the projections perpendicular to the long axis of the nanorod. All five subcrystals in this case have a 180° rotational difference from the referenced one, and they can yield the same electron diffraction patterns. The three possible orientations for the pentatwinned rod are related by a rotation of 18° and 36° around the common [110] central axis, and the structural models (see the insets) are therefore confirmed by electron diffraction observations as previously reported for copper nanorods.[6]

HRTEM observations of a single Ag nanorod with a diameter of 20 nm are shown in Figures 3a−b. Fourier spectra (which are equivalent to an optical diffraction patterns) are obtained by the fast-Fourier transformation (FFT) process from three different areas in Figure 3a. Area I, as well as area III, give rise to the diffraction pattern corresponding to the single crystal with FCC structure along the [110] zone axis direction, and area II yields a complicated diffraction pattern containing numerous weak spots. This pattern actually has the same features as illustrated in the SAED pattern of Figure 2b. Moiré fringes mentioned above evidently appear in the area II as clearly shown in the inset. The fringe spacing can be calculated according to the commonly used equations.[17] The distance of the Moiré fringes is about 3.7 Å, consistent with the theoretical calculation from the known equation $D = d1 \cdot d2/d1 - d2$, where $d1 = d_{111}$

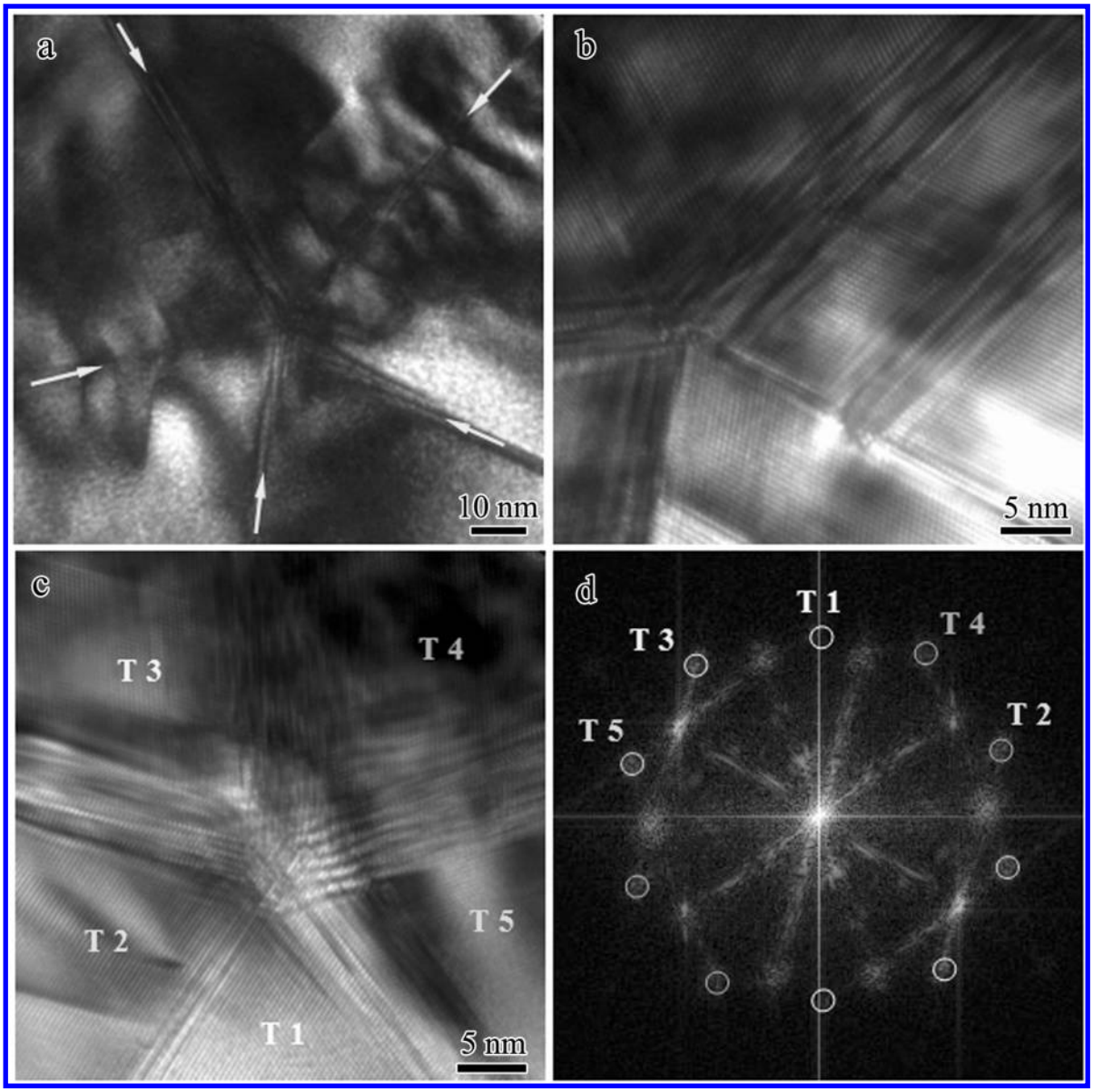

Figure 4. (a) Low-magnification TEM image of the cross-section showing five juxtaposed crystals. (b) HRTEM of the cross-section revealing stacking faults and dislocations along with the twinning boundaries. (c) HRTEM image of the center area of an Ag nanorod cross-section showing five distinctive {111} twinning boundaries. (d) FFT image of Figure 3c showing the same properties as Figure 2a.

and $d2 = d_{220}$. Figure 3b reveals the structural feature at the end of an Ag nanorod, and it demonstrates that the Ag rods grow along the [110] direction with the active (111) crystal plane.

The HRTEM images in Figures. 4a−c show the presence of five distinctive boundaries on the cross-sections of Ag nanorods; the five subcrystals are labeled as T1, T2, T3, T4, and T5, respectively. To get the HRTEM micrographs to reveal the atomic structural feature of the pentagonal sections, we spent a considerable amount of time to find the specific slices of the pentagonal rods that are thin enough (less than 5 nm) for high-resolution imaging. These thin slices are generally perpendicular to the [110] crystallographic zone axis with (111) lattice planes parallel to the twinning boundaries. Figure 4a shows a low-magnitude HRTEM image indicating a clear lattice image of a pentagonal Ag slice (marked by arrows). The different contrasts inside the twinning boundaries are due to the presence of microtwins and stacking faults in the silver matrix. Figures 4b and 4c show the HRTEM images, in which the lattice fringes within Ag subcrystals and near the boundaries can be clearly recognized. The appearance of anomalous contrast fringes in the subcrystals suggests the presence of a high density of stacking faults in addition to the twinning boundaries.[18] These images are taken along the direction perpendicular to the long axis of the rods, so the lattice contrast within each Ag subcrystal can be well understood by the projection of Ag FCC structure along the [110] direction. It is notable that some boundaries are very sharp and result in a well-defined twinning relationship between the twinned subcrystals. On the other hand, a large fraction of the boundaries induces a very complex contrast with evident structural distortions, especially at the core area of the rod. It should also be mentioned that due to the lattice deformation of the Ag subcrystals, the lattice spacings are slightly unequal. This is the same as was mentioned above; in an FCC structure, the interfacial angle between (111) planes is 70.52°. Therefore, it is impossible to perfectly fill the space of a rod by five (111) twinned Ag crystals with only a single-crystalline lattice. The complex contrasts with nearby twinning boundaries are believed to originate from an angular gap of ∼7.4° or wedge Volterra declination.[4] A Fourier spectrum is

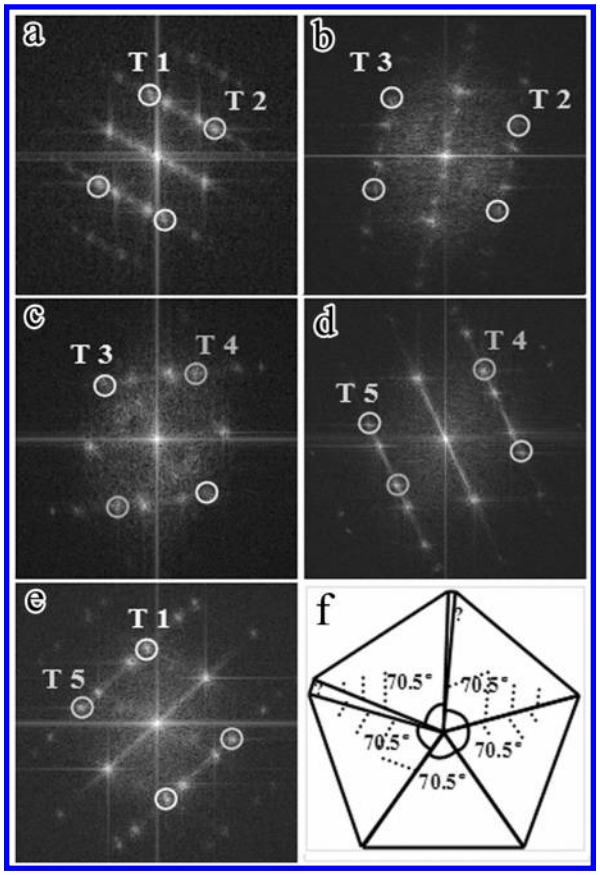

Figure 5. FFT spectra obtained from the boundary areas in the image of Figure 4c. (a), (b), (c), (d), and (e) are obtained from the twinning boundaries of T1 and T2, T2 and T3, T3 and T4, T4 and T5, and T5 and T1, respectively. (f) Pentatetrahedral twin model for an Ag nanorod consistent with our experimental results.

obtained by the FFT process from the center area shown in the Figure 4c HRTEM image. This FFT pattern shows the same symmetric properties as the SAED pattern of the cross-section in Figure 2a.

In previous studies,[5,19] three typical models have been suggested for accommodating the 7.4° gap existing fundamentally in this distinctive kind of fivefold twinned structure, especially in multiply twinned particles: (1) the gap is uniformly accommodated in the multiply twinned particles (MTPs); (2) it is equally assigned among the five twinning boundaries; and (3) the gap is filled on one boundary and results in an incoherent boundary there. When the distortion occurs on one subcrystal to complete the 7.4° gap, the angle in the center for four subcrystals is about 70.5°, while that of the other one is about 77.9°. To directly elucidate the twinning relationship on each boundary, we also obtained statistical data to systematically analyze the spot splitting in FFT spectra from five twinning boundaries.

Figures 5a−e show the FFT spectra obtained from all the twinning boundaries areas shown in the Figure 4c HRTEM image. Figure 5a comes from the twinning boundary area between the T1 and T2 subcrystals. The diffraction spots are sharp, indicating no splitting. It is remarkable that the diffraction spots in Figure 5b show evident splitting, for the spectrum from the twinning boundary between the T2 and T3 subcrystals. Figure 5c shows the spectrum from the twinning boundary between T3 and T4, also yielding light-splitting diffraction spots. The Fourier spectra on twinning boundaries of T4 and T5, as well as T5 and T1, are shown in Figure 5d and Figure 5e, respectively. They both yield sharp spots without observable

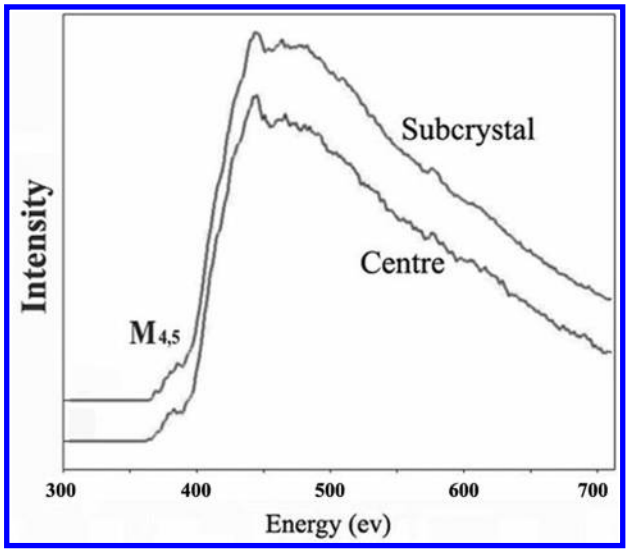

Figure 6. EELS results of the center region in comparison with that from the Ag crystal, electron beam direction along the ⟨110⟩ growth direction.

splitting. According to our HRTEM observations, at least two of five boundaries in general could give rise to recognizable spot splits as discussed above, that is, the 7.4° gap occurring in a pentagonal rod is shared by three boundaries. Based on our experimental results, we propose a new structural model for the cross-section of fivefold twinned nanorods as illustrated in the schematic diagram of Figure 5f. In this model, the coherent gaps occur at least at two twinning boundaries and the angles are apparently different. This feature is possibly connected with the growth mechanism of this kind of nanorod. The dashed lines in the subcrystals of the model (see Figure 5f) indict the presence of typically stacking faults along with twinning boundaries as observed in our experiment shown in Figure 4b.

It is noted that the center of a nanorod is a unique area for all five twinning boundaries in conjunction with the presence of a high density of stacking faults due to the large strain. Hence, further investigations on the defect structures as well as electronic properties in the center region must be the significant issues for understanding the physical properties observed in this kind of thin slice. However, to the best of our knowledge, no theoretical approaches and systematic experimental studies have been performed in previous literatures. To obtain some experimental results on the alternations of electronic structure on the twinning boundaries, we have performed a series of electron energy loss spectroscopy (EELS) examinations on different areas of the cross-section. Figure 6 displays EELS data taken respectively from the center area of the nanorod and a well-crystallized area in a subcrystal using an electron probe of approximately 10-nm diameter. These two spectra for the Ag M-edge show apparent similarity in their general shapes. Careful examinations suggest that the Ag-$M_{4,5}$ peaks from the center area shift to lower energy by a few eV in comparison with results from the Ag subcrystal. Moreover, it must be mentioned that the center area is also distinctive for the atomic arrangement in a local fivefold symmetry, which may partially contribute to the shift of the EELS spectrum. Since understanding the modifications of electronic structure arising from the variation of local atomic arrangement and defects is an important but complex issue, we are only performing a theoretical analysis in comparison with our systemic experimental data. These results will be reported in a coming paper.

Conclusions

In summary, we have systematically investigated the fivefold twinning structure in Ag nanorods. Ag nanorods grown by the polyol-reduction method have a pentagonal shape with the fivefold axis going along the [110] zone axis direction. The remarkable diffraction pattern and HRTEM images obtained from the cross-section observation demonstrate directly that an Ag nanorod has a fivefold twinning structure with five {111} twinned subcrystals. SAED analysis and TEM images of the mature nanorods showed superposition of two specific pairs of crystallographic zones, either [112] and [100] or [110] and [111], which were consistent with a cyclic pentatwinned crystal with five {111} twinning boundaries arranged radially to the [110] direction of elongation. TEM observations along to the rod axis frequently illustrate the additional weak reflections arising from superposition and double-diffraction of twinned subcrystals with evident different orientations. The twinning relationships and local structural distortions on all twinning boundaries have been examined by HRTEM observations and analyzed by FFT processing. Based on our experimental data, we propose a new structural model containing two coherent boundaries for accommodating the strain in this type of pentagonal nanorods. EELS analysis on the center regions of the rods, the unique area with local fivefold atomic symmetry and high density of defects, indicate that the Ag-$M_{4,5}$ peaks shift to lower energy in comparison with results from the Ag crystal.

Acknowledgment. We would like to thank R. J. Xiao, Mr. Y. Q. Zhou, Dr. H. H. Bai, and Mrs. H. L. Fu for their assistance in preparing samples. The work reported here was supported by the ''Hundreds of Talents" program organized by the Chinese Academy of Sciences, P. R. China, and by the ''Outstanding Youth Fund (J. Q. Li)" with Grant No. 10225415.

References and Notes

(1) Hu, J. T.; Odom, T. W.; Lieber, C. M. *Acc. Chem. Res.* **1999**, *32*, 435.
(2) Ino, S. *J. Phys. Soc. Jpn.* **1966**, *21*, 346.
(3) Uyeda, R. *J. Cryst. Growth* **1974**, *24*, 69.
(4) Marks, L. D.; Smith, D. J. *J. Cryst. Growth* **1981**, *54*, 425.
(5) Marks, L. D. *Rep. Prog. Phys.* **1994**, *57*, 603.
(6) Urban, *J. Cryst. Res. Technol.* **1998**, *33*, 1009.
(7) Lisiecki, I.; Filankembo, A.; Sack-Kongehl, H.; Weiss, K.; Pileni, M.-P.; Urban. *J. Phys. Rev. B* **2000**, *61*, 4968.
(8) Hofmeister, H.; Nepijko, S. A.; Ievlev, D. N.; Schulze, W.; Ertl, G. *J. Cryst. Growth* **2002**, *234*, 773.
(9) Cepak, V. M.; Martin, C. R. *J. Phys. Chem. B* **1998**, *102*, 9985.
(10) Zhou, Y.; Yu, S. H.; Cui, X. P.; Wang, C. Y.; Chen, Z. Y. *Chem. Mater.* **1999**, *11*, 545.
(11) Zhu, J.; Liu, S.; Palchik, O.; Koltypin, Y.; Gedanken, A. *Langmuir* **2000**, *16*, 6396.
(12) Xia, Y. N.; Yang, P. D.; Sun, Y. G.; Wu, Y. Y.; Mayers, B.; Gates, B.; Yin, Y. D.; Franklin, K.; Yan, H. Q. *Adv. Mater.* **2003**, *15*, 353.
(13) Sun, Y. G.; Mayers, B.; Herricks, T.; Xia, Y. N. *Nano Lett.* **2003**, *3*, 955.
(14) Gao, Y.; Jiang, P.; Liu, D. F.; Yuan, H. J.; Yan, X. Q.; Zhou, Z. P.; Wang, J. X.; Song, L.; Liu, L. F.; Zhou, W. Y.; Wang, G.; Wang, C. Y.; Xie, S. S. *Chem. Phys. Lett.* **2003**, *380*, 146.
(15) Nepijko, S. A.; Levlev, D. N.; Schulze, W.; Urban, J.; Ertl, G. *ChemPhysChem* **2000**, *3*, 140.
(16) Pauwels, B.; Bernaerts, D.; Amelinckx, S.; Van Tendeloo, G.; Joutsensaari, J.; Kauppinen, E. I. *J. Cryst. Growth* **1999**, *200*, 126.
(17) Edington, J. W. *Practical Electron Microscopy in Materials Science*; TechBooks: Herndon, **1976**.
(18) Hillebrand, R.; Hofmeister, H.; Scheerschmidt, K.; Heydenreich, J. *Ultramicroscopy* **1993**, *49*, 252.
(19) Wu, Y.; Chen, Q.; Takeguchi, M.; Furuya, K. *Surf. Sci.* **2000**, *462*, 20.